Inorg. Chem. **2008**, *47*, 5558−5560

Synthesis of Superparamagnetic β-MnO_2 Organosol: a Photocatalyst for the Oxidative Phenol Coupling Reaction

Subhra Jana, Surojit Pande, Arun Kumar Sinha, and Tarasankar Pal*

Department of Chemistry, Indian Institute of Technology, Kharagpur 721302, India

Received March 19, 2008

Superparamagnetic monodispersed spherical β-MnO_2 nanoparticles of ~10 nm size with a band gap of 2.52 eV have been synthesized in toluene and support the oxidative phenol coupling reaction as a photocatalyst.

During the last few decades, nanoparticles of transition-metal oxides have received steadily growing importance not only for their fundamental scientific significance but also for many technological applications.[1] Large surface-to-volume ratio and surface atomic activity make the nanoparticles attractive catalysts compared to bulk materials.[2] The recent research has been devoted to the synthesis of well-defined monodispersed metal and semiconductor nanoparticles in organic media for their applications in catalysis, spectroscopy, and printed electronics.[3] Because most of the reactions are carried out in an organic phase, it is desirable to synthesize the catalyst particles in an organic solvent in lieu of hydrosol.

Manganese oxides have been extensively investigated as catalysts, ion exchangers, soft magnetic materials, and electrode materials in Li/MnO_2 batteries, and their performance is highly dependent on their morphology as well as crystallographic forms.[4] They have been used for a wide range of industrial catalytic applications, such as ozone decomposition, photocatalytic oxidation of organic pollutants, nitric oxide reduction, selective oxidation of carbon monoxide, decomposition of hydrogen peroxide, and so on.[5] A wide variety of structural forms of manganese dioxide, α, β, γ, and δ types, have been reported, where the basic structural octahedral unit [MnO_6] linked in different ways.[4]

The syntheses of metal nanoparticles in an aqueous system are easy to manipulate because of the high dielectric constant of the medium that helps a variety of ions and stabilizer molecules such as surfactants, polymers, and coordinating ligands for solubilization.[6] In spite of the great advantages of water-based synthesis, there are some inherent problems, e.g., stabilizer residue removal after synthesis, difficulty in surface modifications of nanoparticles, increases in particle concentrations, etc.[7] Furthermore, owing to the high surface energy of the nanoparticles, they have the tendency to agglomerate, which hinders their synthesis in high concentration in aqueous solution.[8] In contrast, particles synthesized in organic solvents might be a promising solution to all of these problems.[9] To the best of our knowledge, there is no report of a straightforward synthesis of MnO_2 nanoparticles strictly in an organic solvent.

In this Communication, we have reported for the first time a facile and homogeneous reduction technique for the synthesis of monodispersed β-MnO_2 nanoparticles in an organic solvent. The particles exhibit no sign of aggregation even after 6 months. The particles were characterized by different physical methods and display a band gap of 2.52 eV and strong oxidation at 1.12 V. Their magnetic properties have also been investigated in depth. Finally, the particles have been employed as a photocatalyst for the synthesis of a coupled product of β-naphthol.

MnO_2 organosol has been synthesized by exploiting a two-phase (water−toluene) extraction procedure. At first, an aqueous solution of $KMnO_4$ (5 mL, 10 mM) and 50 mL of toluene were taken together in a 100 mL separating funnel. Then, 25 mg of tetra-*n*-octylammonium bromide (TOAB), a phase-transfer reagent, was introduced into this mixture and shaken vigorously. As a consequence, MnO_4^- was transferred from the aqueous phase to the organic layer, leaving behind a colorless aqueous solution. Now, upon the

* To whom correspondence should be addressed. E-mail: tpal@chem.iitkgp.ernet.in.

(1) Burda, C.; Chen, X. B.; Narayanan, R.; El-Sayed, M. A. *Chem. Rev.* **2005**, *105*, 1025.
(2) (a) Alivisatos, A. P. *Science* **1996**, *271*, 933. (b) Lee, G. H.; Huh, S. H.; Jeong, J. W.; Choi, B. J.; Kim, S. H.; Ri, H. C. *J. Am. Chem. Soc.* **2002**, *124*, 12094. (c) Narayanan, R.; El-Sayed, M. A. *J. Am. Chem. Soc.* **2003**, *125*, 8340.
(3) Li, Y.; Wu, Y.; Ong, B. S. *J. Am. Chem. Soc.* **2005**, *127*, 3266.
(4) (a) Thackeray, M. M. *Prog. Solid State Chem.* **1997**, *25*, 1. (b) Jana, S.; Praharaj, S.; Panigrahi, S.; Basu, S.; Pande, S.; Chang, C. H.; Pal, T. *Org. Lett.* **2007**, *9*, 2191.
(5) (a) Zhang, L. C.; Liu, Z. H.; Tang, X. H.; Wang, J. F.; Ooi, K. *Mater. Res. Bull.* **2007**, *42*, 1432. (b) Feng, Q.; Kanoh, H.; Ooi, K. *J. Mater. Chem.* **1999**, *9*, 319.
(6) (a) Wei, G.-T.; Yang, Z.; Lee, C.-Y.; Yang, H.-Y.; Wang, C. R. C. *J. Am. Chem. Soc.* **2004**, *126*, 5036. (b) Huang, S.; Ma, H.; Zhang, X.; Yong, F.; Feng, X.; Pan, W.; Wang, X.; Wang, Y.; Chen, S. *J. Phys. Chem. B* **2005**, *109*, 19823.
(7) (a) Goia, D. V.; Matijevic, E. *New J. Chem.* **1998**, *22*, 1203. (b) Kim, K.-S.; Demberelnyamba, D.; Lee, H. *Langmuir* **2004**, *20*, 556.
(8) Nath, S.; Ghosh, S. K.; Praharaj, S.; Panigahi, S.; Basu, S.; Pal, T. *New J. Chem.* **2005**, *29*, 12.
(9) Gittins, D. I.; Caruso, F. *Angew. Chem., Int. Ed.* **2001**, *40*, 3001.

10.1021/ic800499q CCC: $40.75
Published on Web 06/12/2008

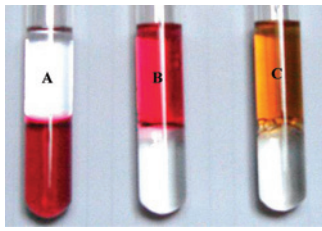

Figure 1. Photograph of an aqueous $KMnO_4$ solution with toluene (A), MnO_4^- transferred to toluene (B), and organosol of MnO_2 in toluene (C).

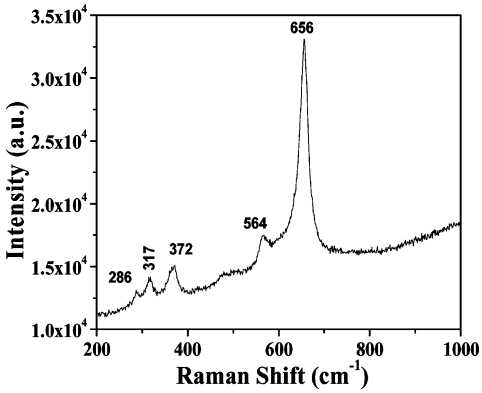

Figure 2. RS of MnO_2 organosol at room temperature.

addition of 5 mg of tetrabutylammonium borohydride ($TBABH_4$) to this organic phase and on vigorous shaking, the purple color of the solution becomes brown, which indicates the onset of the evolution of MnO_2 nanoparticles in toluene (Figures 1 and S4 in the Supporting Information). The particles remain stable for months together. The as-synthesized nanoparticles were dried using a rotary evaporator, and the solid mass was redispersed in toluene and other nonpolar organic solvents, where it showed no aggregation.

The powder X-ray diffraction (XRD) pattern of the as-synthesized product, MnO_2 organosol does not show any crystallinity because of TOAB capping. However, the XRD pattern of the product exhibits some well-defined peaks when TOAB is removed (Figure S1 in the Supporting Information). All of the diffraction peaks of the particles can be readily indexed to a pure tetragonal phase of β-MnO_2 (JCPDS Card, No. 24-0735, $a = 4.399$ Å and $c = 2.874$ Å) with space group $P4_2/mnm$. The binding energies obtained in the X-ray photoelectron spectroscopy (XPS) analysis were corrected for specimen charging by referencing C 1s to 286.2 eV. Figure S2 in the Supporting Information shows a doublet consisting of two components centered at binding energy values of 642.37 eV (Mn $2p_{3/2}$) and 653.71 eV (Mn $2p_{1/2}$), which are characteristic of $Mn^{IV}O_2$.[10]

Raman spectroscopy is a powerful experimental technique for the identification and characterization of the local Mn environment, which further authenticates the particles as β-MnO_2. Organosol of MnO_2 in the β phase indicates a very strong and well-defined Raman peak (Figure 2) in the nanodomain. A similar observation has been reported for

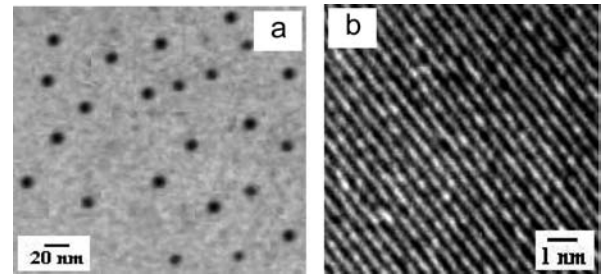

Figure 3. TEM (a) and HRTEM (b) images of MnO_2 organosol.

β-MnO_2 hydrosol.[11] The spectrum shows a strong sharp peak located at 656 cm^{-1} and a weak band at 564 cm^{-1} along with three weak peaks located at 372, 317, and 286 cm^{-1}. The main contributions are attributed to the stretching mode of $[MnO_6]$ octahedra. The corresponding antisymmetric stretching modes are recorded in the FTIR spectrum at 518 and 669 cm^{-1} (shown in Figure S3 in the Supporting Information). RS peaks at lower wavenumbers are attributed to the deformation modes of the metal−oxygen chain of Mn−O−Mn in the MnO_2 octahedral lattice.

The size distribution, morphology, and crystallographic structure of β-MnO_2 organosol were investigated by transmission electron microscopy (TEM). Figure 3a represents the TEM image of spherical β-MnO_2 nanoparticles with an average particles size of 10 ± 1 nm. The particles are well separated from the neighboring nanoparticles, indicating the surface passivation and steric stabilization of the nanoparticles by TOAB molecules. The fringe spacing (0.398 nm) observed in the high-resolution TEM (HRTEM) image (Figure 3b) agrees well with the separation between (110) lattice planes.

It has been documented that the nanoparticles of larger sizes were believed to grow at the expense of smaller ones via the Ostwald ripening process, where small nanoparticles dissolved and grew into larger crystals.[12] The crystal growth and dissolution of nanoclusters occurred simultaneously. Therefore, the formation of uniform and well-shaped particles can be accounted for as a consequence of the balance between stabilization and crystal growth in a low dielectric solvent. Because of the large surface-to-volume ratio of the nanosized particles, the dissolution becomes easier and the growth rate is comparatively slower because small particles often grow more rapidly than macrocrystals.[13] Consequently, a uniform size distribution is obtained at the end, which is a general characteristic habit of organosol,[8] unlike the hydrosol of MnO_2, where unidirectional growth becomes the usual phenomenon.[4,14]

The addition of TOAB to the aqueous phase resulted in a swift movement of MnO_4^- to the toluene layer because of the formation of ion pair $[TOA]^+[MnO_4]^-$. As a result, the organic layer becomes purple. Upon the addition of $TBABH_4$ into the organic layer, the purple color gradually disappears and a brown color develops. This is due to the onset of the evolution of MnO_2 nanoparticles under the homogeneous

(10) Wanger, C. D.; Riggs, W. M.; Davis, L. E.; Moulder, J. F.; Muilenberg, G. E. *Handbook of X-ray Photoelectron Spectroscopy*; Perkin-Elmer: Eden Prairie, MN, 1978.

(11) Jana, S.; Basu, S.; Pande, S.; Ghosh, S. K.; Pal, T. *J. Phys. Chem. C* **2007**, *111*, 16272.

(12) Shen, Z.; Zhao, Z.; Peng, H.; Nygren, M. *Nature* **2002**, *417*, 266.

(13) Mullin, J. W. *Crystallization*, 3rd ed.; Butterworth Heinemann: Woburn, MA, 1997; p 172.

(14) Wang, X.; Li, Y. L. *J. Am. Chem. Soc.* **2002**, *124*, 2880.

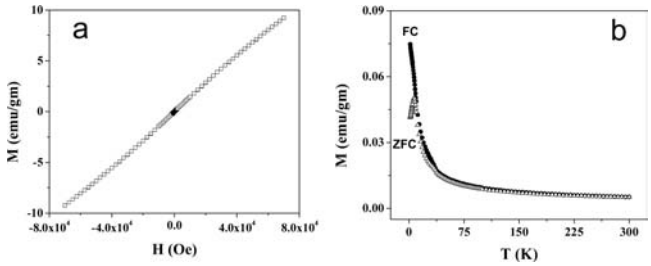

Figure 4. Field-dependent magnetization curve at 40 K (a) and a magnetization vs temperature curve at an applied field 100 Oe (b).

reduction procedure (spectral information in Figure S4 in the Supporting Information authenticates all of the facts). Here, $TBABH_4$ is introduced in lieu of $NaBH_4$ to avoid precipitation. The stability of the nanoparticles in solution arises from the electrostatic repulsion because of their surface charge. Here, tetraoctylammonium ions are adsorbed onto the surface of MnO_2 nanoparticles, creating a surface charge that stabilizes the particles. The particles retain their unchanged morphology for a long time in varied organic solvents without any sign of agglomeration.

The magnetic properties of β-MnO_2 nanoparticles were studied by a SQUID magnetometer. Magnetic anomalies, such as low-temperature hysteresis below a blocking temperature and divergence between field-cooling (FC) and zero-field-cooling (ZFC) magnetization data, of β-MnO_2 nanoparticles have been demonstrated here. The anomalies in the magnetic properties are attributed to uncompensated surface spins, causing a changein the magnetic order in the nanoparticles.[15] Figure 4a displays a field dependence magnetization curve of β-MnO_2 organosol at 40 K, which indicates a superparamagnetic state at this temperature, because the coercive force and remnant magnetization are zero. At 2 K temperature, the particles show ferromagnetic behavior having a small hysteresis with a coercive force of 537 Oe and remnant magnetization of 0.504 emu/g compared to bulk MnO_2, which shows antiferromagnetic behavior at low temperature (Figure S6 in the Supporting Information). The temperature-dependent magnetization curves under ZFC and FC conditions at 100 Oe have been presented in Figure 4b. The ZFC curve clearly shows a maximum corresponding to the blocking temperature (T_B) of the nanoparticles, which has been calculated to be 7 K. The FC and ZFC data show divergence at low temperature, as is indeed found in the case of other oxide nanoparticles.

For a superparamagnet, hysteresis is observed below the blocking temperature. Above the blocking temperature, the temperature overcomes the particle anisotropy energy barrier and they behave as paramagnets with a very high magnetic moment: they are said to be unblocked. Therefore, at higher temperature ($T > T_B$), hysteresis disappears. However, it is already established that, because of the confinement in the nanoscale, nanomaterials can exhibit unusual magnetic behavior that is quite different from those of conventional bulk materials and their magnetic properties are highly sensitive to the size and shape. Earlier, we have reported the synthesis of ~5 nm MnO_2 nanospheres with a T_B of 40 K.[11] However, in the present case, T_B of the 10 nm particles is 7 K. So, it becomes interesting to note that T_B for smaller particles becomes higher than that of larger ones, indicating an inverse relationship.

The as-synthesized β-MnO_2 organosol has become successful as an effective photocatalyst for C−C bond formation, initiating an oxidative phenol coupling reaction between β-naphthol moieties at room temperature. A toluenic solution of β-naphthol (10 mL, 10^{-2} M) and β-MnO_2 organosol (200 μL, 10^{-3} M) were introduced in a glass reaction vessel. Then the reaction mixture was irradiated under visible light (60 W tungsten lamp) for 12 h. The exclusive product, binol (67%, quantum yield 0.27), was isolated by column chromatography using petroleum ether−ethyl acetate (10:1) as an eluant and was characterized via thin-layer chromatography and NMR studies. The reaction scheme[16] is given below:

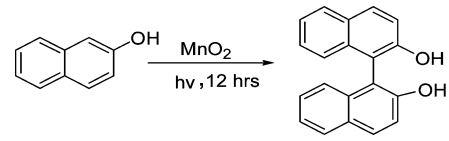

In the dark, the reaction does not proceed. It has also been observed that commercially available MnO_2 could not produce binol under the same reaction protocol even after 24 h. The catalytic activity of β-MnO_2 organosol resulting from its larger surface area, active surface sites, tenacious moisture retention capacity,[17] and photon absorption (~400 nm) capability in the visible region[18] is proved beyond doubt. It has also been observed that the yield of the product is enhanced (14%) in the presence of benzoyl peroxide (0.1 mM) and drastically reduced (~2%) when hydroquinone (0.1 mM) is introduced into the reaction mixture. This advocates a free-radical mechanism under illumination.

In conclusion, we demonstrate a homogeneous reduction route for the synthesis of semiconductor β-MnO_2 organosol. The particles are stable for months together and redispersible in different organic solvents. This is a very simple, facile, and reproducible approach for gram level synthesis of MnO_2 nanoparticles in organic solvents and hence is deliverable. The particles exhibit superparamagnetism, accompanied by magnetic hysteresis below the blocking temperature of 7 K. Finally, the particles have been successfully exploited as an efficient photocatalyst for oxidative phenol coupling reaction.

Acknowledgment. This work was supported by CSIR, UGC, DST, New Delhi, and IIT−Kharagpur.

Supporting Information Available: XRD, XPS, FTIR, cyclic voltammogram, and UV−visible spectra and characterization of binol. This material is available free of charge via the Internet at http://pubs.acs.org.

IC800499Q

(15) (a) Kodama, R. H. *J. Magn. Magn. Mater.* **1999**, *200*, 35. (b) Kodama, R. H.; Makhlouf, S. A.; Berkowitz, A. E. *Phys. Rev. Lett.* **1997**, *79*, 1393.

(16) Guo, Q.-X.; Wu, Z.-J.; Luo, Z.-B.; Liu, Q.-Z.; Ye, J.-L.; Luo, S.-W.; Cun, L.-f.; Gong, L.-Z. *J. Am. Chem. Soc.* **2007**, *129*, 13927.

(17) Cook, M. J.; Forbes, E. J.; Khan, G. M. *Chem. Commun.* **1966**, 121.

(18) (a) Wang, L.; Ebina, Y.; Takada, K.; Sasaki, T. *Chem. Commun.* **2004**, 1074. (b) Brock, S. L.; Sanabria, M.; Suib, S. L. *J. Phys. Chem. B* **1999**, *103*, 7416.